IGM88TC-404-733-G
CNRC 28912

OPTICAL INSPECTION OF SHEET MATERIAL FOR PINHOLES OR DEFECTS BY SPECKLE-AVERAGING TECHNIQUES

by P. Cielo and G. Vaudreuil
National Research Council Canada
Industrial Materials Research Institute
75 De Mortagne Blvd., Boucherville, Québec J4B 6Y4 Canada

ABSTRACT

Techniques for defect detection by stationary laser line projection and wide-area light detection are described. Diode laser line-arrays are used, when possible, to relax safety requirements and reduce speckle noise by incoherent superposition.

INTRODUCTION

Continuous on-line inspection of a moving sheet is one of the most active fields of optical inspection. Examples of sheet materials for which optical inspection systems have been reported include paper webs, plastics sheets, textile fabric, glass material, hot slabs and cold-rolled metal strips (Ref. 1, Sect. 4.3.2). These systems are an essential tool for modern statistical process control procedures.

Different optical configurations can be used for these applications, including laser scanning, linear array electronic imaging or 2-D camera inspection in either a reflecting, a transmissive, a retroreflecting or a scattering setup. Several optomechanical and electro-optical design choices will be analyzed in this paper with reference to a number of inspection tasks in which our institute was recently involved. The emphasis is on design choices leading to a consistently high signal-to-noise ratio, extended system lifetime with low maintenance costs, and minimization of eye safety requirements.

GENERAL CONDISERATIONS

Figure 1 shows a typical on-line sheet inspection system. The system scans in a cross-machine direction the continuously moving web for a 100 percent inspection. Either reflection or transmission configurations are possible, depending on whether an opaque or a transparent sheet is to be inspected. Defects corresponding to spots of abnormal reflectivity or transmissivity are recorded and kept in memory, or else a spray marker may be used to facilitate defect localization for further processing.

Cross-machine scanning may be implemented either mechanically or electronically. An example of a mechanically scanned laser inspection system is shown in Fig. 2[2, 3]. The laser beam is angularly scanned by a rotating polygon and the light scattered back from the strip is detected by an optical receiver containing a diffusing-cavity photomultiplier. Laser mechanical scanning has the advantages of providing a high brightness illumination, large depth of field and the possibility of sharp spectral filtering. However, sequentially scanning systems result in very short pixel dwell times, thus requiring large-bandwidth detectors with correspondingly lower signal-to-noise ratios. Another problem of laser scanning is the presence of speckle noise (Ref. 1, Sect. 3.10). Finally, and most importantly, the requirement for high-speed rotating parts decreases the ruggedness and the lifetime of mechanically scanned systems. Nonmechanical laser scanning devices such as acousto-optical deflectors are severely limited in terms of deflection angles and angular resolution (Ref. 1, Sect. 3.8).

Electronic scanners using stationary light sources and staring detector arrays are being increasingly favored by industrial inspection instrumentation manufacturers. The absence of moving parts is very much appreciated in hostile industrial environments, while earlier detector array drawbacks such as limited scanning speeds, pixel-to-pixel nonuniformity and reduced dynamic range[4, 5] are being substantially reduced by the recent availability of high-quality and inexpensive detector arrays. A typical reflection mode, staring-array inspection system using line illumination and linear array imaging is shown in Figure 3[6].

High-power linear lamps are normally used across the moving web to provide a sufficiently bright illumination[7]. Laser illumination would be more convenient in terms of brightness, depth of field and spectral filtering capabilities as mentioned above. Moreover, modern diode lasers are more compact and have a much longer lifetime than conventional lamp sources, while the laser directionality makes it possible to select a specific angular scattering range to improve defect detectability, as will be discussed below. Techniques for line-array scanning a laser-illuminated sheet will be described in this paper, and methods to reduce coherent spatial noise as well as eye safety concerns will be discussed.

CONSTANT-INCIDENCE SCANNING

An aspect which does not always receive proper consideration in surface scanning systems for defect detection is the angular distribution of the light scattered by the defect. Angular properties are of primary importance when defects are defined in terms of their microstructural morphology, such as scratches or pits in metal sheets, rather than in terms of their light absorbing characteristics, such as black spots on a paper web.

The importance of angular considerations when optically inspecting smooth surfaced sheets is well exemplified in Figure 4. This graph shows the scattered light intensity from a surface discontinuity defect on a glass sample, experimentally recorded with a transmission version of the setup shown in Figure 3. It can be concluded from this curve that defects which are clearly visible at low scattering angles may give signals smaller by several orders of magnitude when viewed at larger angles from the unscattered light beam. This makes Bayesian thresholding (Ref. 1, Fig. 4-37) quite difficult in circumstances of this kind. It should also be noted at this point that a conventional diffuse illumination using incoherent lamps is inappropriate for this kind of defects whose angular scattering characteristics are essential for defect enhancement.

The requirement for nearly constant projection and viewing angles to avoid strong variations of scattering efficiency has already been mentioned in relation with the laser inspection of materials such as metal sheets (Ref. 1, Sect. 4.3.2). A possible approach for constant-angle scanning is to use a wide-aperture cylindrical mirror, as shown in Figure 5[11]. A less cumbersome configuration using Fresnel lenses was recently investigated at our institute. As shown in Figure 6, a diverging laminar beam is collimated by a Fresnel lens to be projected on the glass sheet at a constant angle. Plastics-molded Fresnel lenses are convenient for industrial installations because of their low weight and volume even at diameters close to 1 m. Their relatively important aberrations do not constitute a problem for this kind of applications. After transmission through the glass, the beam is focused by a second Fresnel lens on the entrance pupil of a line-array camera which is focused on the glass sheet. If a scattering defect is present anywhere along the illuminated line (dotted lines in Figure 6), the scattered beam will always be centered on the camera. The visibility of a defect is thus constant no matter its position along the projected line.

As shown by the insert in Figure 6, Fresnel lenses are characterized by a series of indentations, which act as scattering discontinuities similarly to the scattering defects on the glass. This is the reason why the line-array output shown in Figure 7 presents large signal excursions even in the absence of scattering defects on the glass. Figure 8(a) shows an enlarged portion of the light level excursions produced by the Fresnel lens indentations, as recorded by a detector array located at 90 mm from the lens. Such excursions become more regular at the Talbot imaging planes (see, e.g., Ref.6, Fig. 51), as shown in Figure 8(b). Such planes are located at distances from the lens equal to multiples of $2p^2/\lambda$, where p is the lens indentation period and λ is the wavelength. If the glass sheet can be placed in one of these planes, the lens-produced modulation can be substantially reduced by using two suitably spaced light sources, as Figure 8(c) shows.

If the geometrical alignment requirements described above cannot be met, a dynamic reference approach can be chosen to smoothen out the detector array output. Dynamic referencing is a convenient technique for suppressing repetitive noise, as it is the case for the modulation noise introduced by the Fresnel lenses in our case. As shown in Figure 9, the signal modulation introduced by the lens indentations is constant as the glass sheet moves. By taking the difference between the signals corresponding to a defect-free portion and a portion with a defect, the presence of the defect is enhanced by suppressing the constant-modulation noise. This approach can be conveniently implemented by keeping in memory a reference corresponding to a defect-free portion to continuously normalize the output signal. By continuously updating the reference, e.g. by keeping in memory the average of the last 1000 line scans, one can suppress as well the effects of a slowly variable background such as the presence of stray light in the inspection environment.

The constant-incidence configuration is convenient not only in a transmission design of the kind shown in Figure 6, but also in a scattering configuration. A small-angle scattered light detecting system, which is particularly suited to the detection of nonabsorbing

defects in presence of strong ambient vibration, is shown in cross-section in Figure 10. In this case only light scattered by defects on the glass panel is allowed to reach the camera, resulting in dark-background signals of the kind shown in Figure 11. The scattering angle was a constant 10 degrees from the transmitted beam in this case. With reference to Figure 4 above, it can be seen that the defect visibility increases if small values of the scattering angle are chosen. This example clearly shows the importance of choosing a well collimated laser source as opposed to a diffuse illumination, as well as of adopting a constant-incidence design, when small-angle scattering defects must be detected.

Finally, it should be mentioned that electro-optical configurations of the kind shown in Figures 6 or 10 are practical in terms of both maintenance and safety considerations. Maintenance requirements are reduced by the choice of laser-diode line illuminators: apart from the longer lifetime of laser diodes compared to incoherent lamp sources, this approach simplifies the design of air purging enclosures to keep the optics clean. Indeed, both illumination and imaging can be performed through narrow, typically 1 mm-wide, slits which are particularly well suited to air purging. On the other hand, the distribution of the laser power over a long line reduces the power density over the eye of an observer even if he is allowed to view directly the collimated laminar beam, so that safety concerns are relaxed. These two combined features make laminar laser beam illumination more advantageous than either laser scanning or incoherent two-dimensional illumination for this kind of applications.

PINHOLE DETECTION

A setup substantially similar to the one shown in Figure 6 may be used to detect defects other than scratches on transparent panels. One application with which we have become recently involved is the on-line detection of pinholes on metal sheet material, and more particularly the measurement of pinhole density on aluminum foil. Pinholes as small as 10 μm in diameter must be detected in this case at sheet speeds reaching 10 m/s.

The chosen configuration for pinhole detection and counting is shown in Figure 12. As in the case of Figure 6, a nearly collimated laminar beam is projected across the moving sheet, and the transmitted light power is collected on an optical detector. However, in the system illustrated in Figure 12 a single, wide-area detector is used to reach a higher response speed and sensitivity to minute pinholes. As only the density, and not the position of the pinholes are to be recorded in this case, a segmented line-array detector is not required. Using a single detector is more effective in this case because of its higher speed and sensitivity, as described below.

The choice of a single sensor enables the optical designer to choose a highly sensitive device, such as an avalanche photodiode, while its sensitive surface may be expanded to collect the full image of the pinhole to be detected, giving a signal level which is higher than the level obtained from the individual sensors of a line-array photodetector. Moreover, the maximum allowed sheet speed is practically unlimited in the case of Figure 12: if a narrow laminar beam of 1 mm-width is projected across a sheet travelling at 10 m/s, the beam-crossing time period for the pinhole is of the order of 100 μs. Such a response speed is very easily met by a single photodetector, while being at the limit of the scanning speed for a large line-array device. Finally, differential double-detection schemes are easier to implement with single sensors. As shown in Figure 12, two detectors may be used to selectively collect light of different wavelengths or polarizations by using a suitable optical filter BS. By matching the filter transmissivity to the wavelength or polarization of the laser source, and taking the ratio of the outputs from the two detectors, light transmitted by pinholes may be effectively differentiated from, e.g., ambient light scattered by a scratch defect passing through the field of view of the detector.

A further interest of a single-sensor detection is the possibility of time-filtering the detector output to enhance defect recognition. As the pinhole travels through the narrow projected laminar beam, a short pulse is recorded by the detector with a pulse shape and duration which is determined by the known sheet speed and light distribution across the projected laser line. By using an electronic filter matched to such a pulse shape, the selectivity of the pinhole detection system over ambient or electronic noise can be considerably enhanced. Figure 13 shows a computer simulation of the signal detected with a system of the kind shown in Figure 12 when the projected light pattern is shaped to either a $\sin^2 x/x^2$ distribution, as obtained by inserting a slit mask along the laser beam, or an interference fringe pattern as obtained with a beam-splitting device of the kind used in laser Doppler anemometry. By deconvoluting the signal + noise waveforms shown in Figure 13(b) with the corresponding waveforms (a), the signal visibility is considerably enhanced, as shown in Figures 13(c) and (d).

A pinhole counting sensor of the kind described above was mounted on an aluminum foil parting machine of which a general view is shown in Figure 14. Aluminum foil lengths of

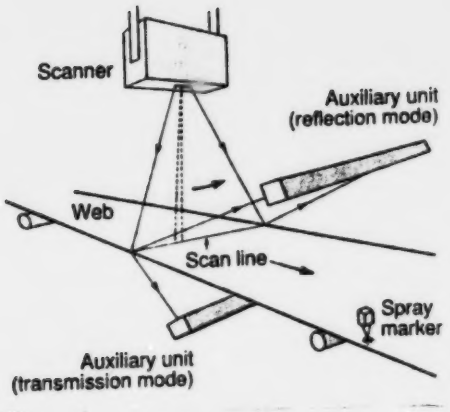

Figure 1: Typical configuration for an industrial laser web-scanning optical inspection system.

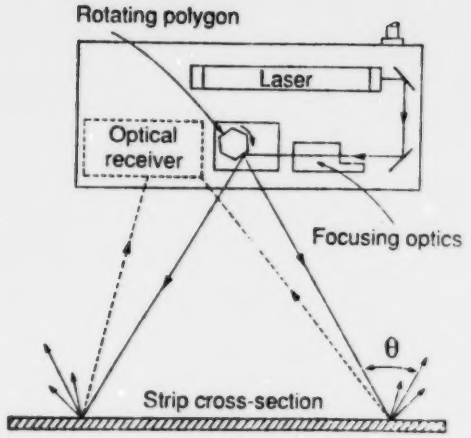

Figure 2: Laser-scanning device for surface inspection across a strip.

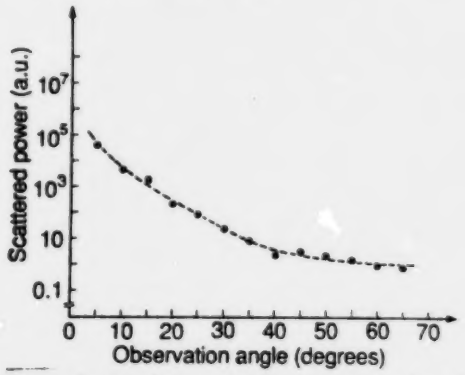

Figure 4: Angular scattering spectrum from a surface defect on a glass panel.

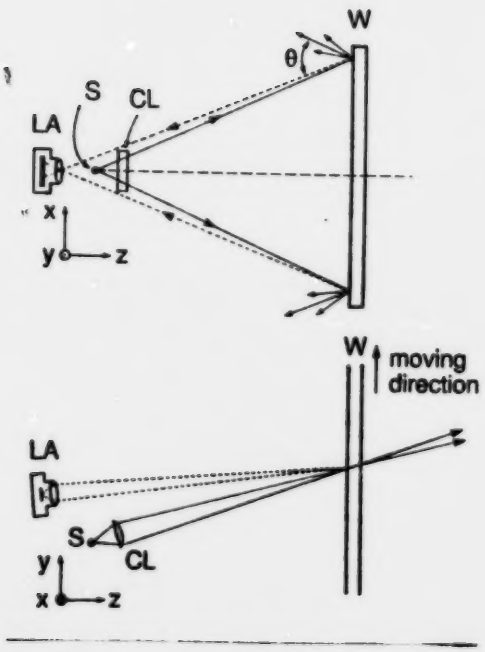

Figure 3: Electronically scanning inspection system using laminar light beam projection and line-array camera imaging.

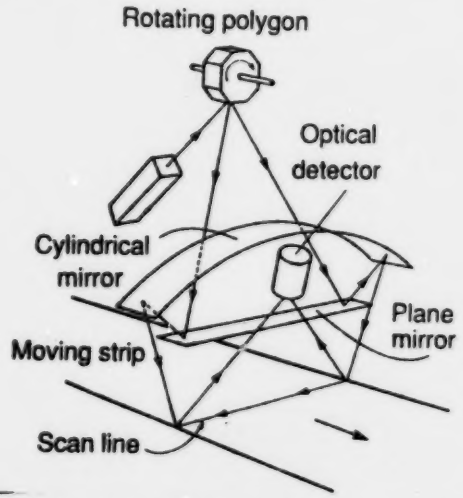

Figure 5: Constant-angle viewing geometry for laser scanning a metallic strip.

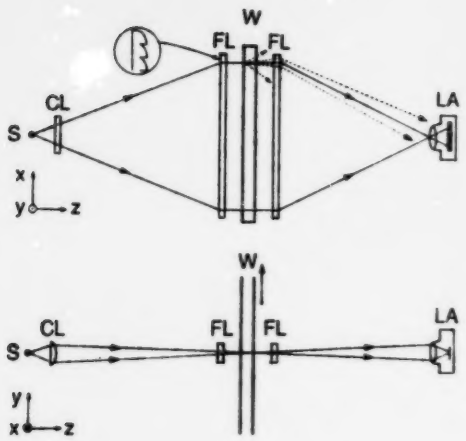

Figure 6: A constant-angle, transmission configuration for the detection of scattering defects on a transparent panel. S: light source; FL: Fresnel lenses; W: transparent sheet; LA: linear array camera.

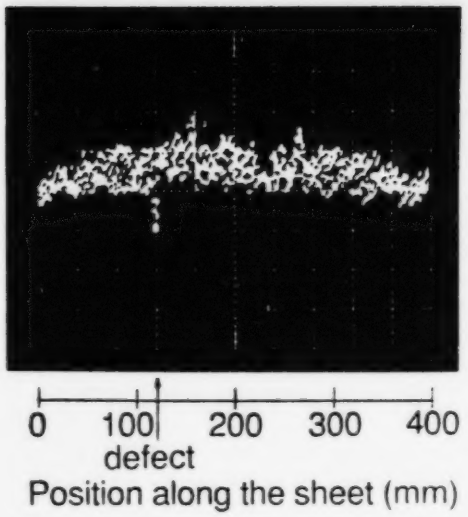

Figure 7: Unprocessed output from the line-array camera as obtained with the setup shown in Figure 6. Note the large signal excursion due to Fresnel lens diffraction effects.

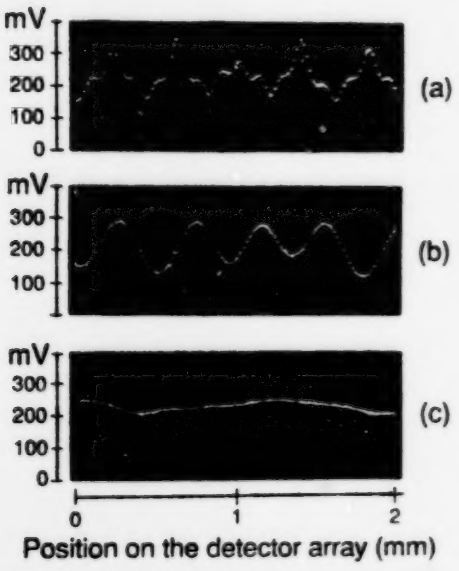

Figure 8: Enlarged portion of the signal recorded with an array detector directly located at a distance of (a) 90 mm and (b) 220 mm from the Fresnel lens. Signal (c) was obtained as in (b), but using two suitably spaced laser sources to reduce the lens-produced modulation.

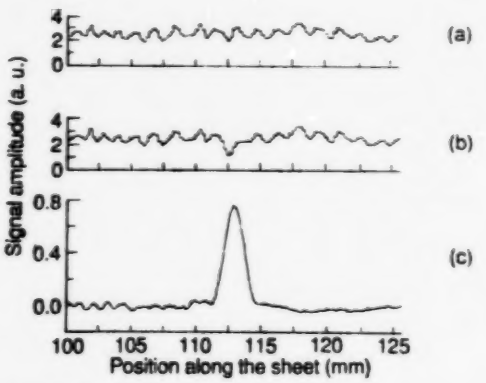

Figure 9: Line-array image of a portion of the glass (a) without defects and (b) with a defect; signal (c) is the low-pass filtered difference (a)-(b).

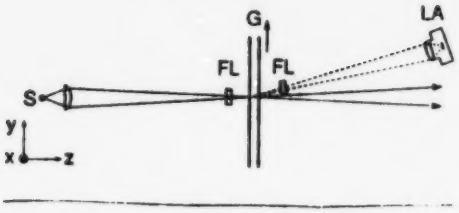

Figure 10: Constant-incidence configuration similar to the one shown in Figure 6 but giving a dark-background output.

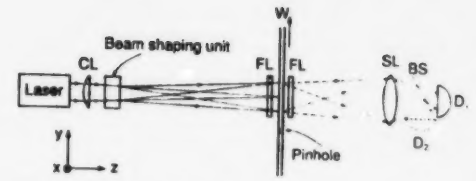

Figure 12: Cross-sectional diagram of an optical system similar to the one shown in Figure 6, but using a single sensor to detect pinholes on a moving sheet. W is the sheet, D_i are sensors and BS is a selective beam splitter, while CL, FL and SL indicate, respectively, cylindrical, Fresnel and spherical lenses.

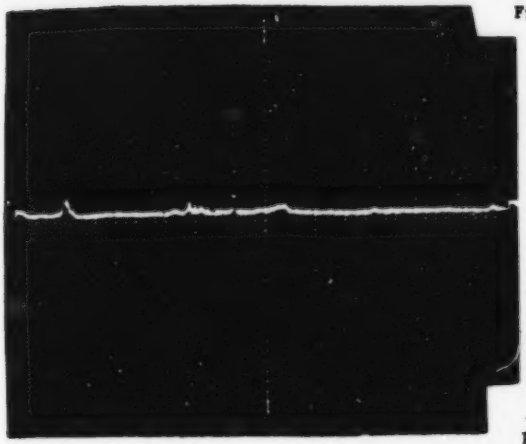

Figure 11: Dark-background signal obtained with a setup of the kind shown in Figure 10. A scattering defect (small air bubble within the glass) is visible near the middle of the scanned line. Vertical scale: 200 mV/div.

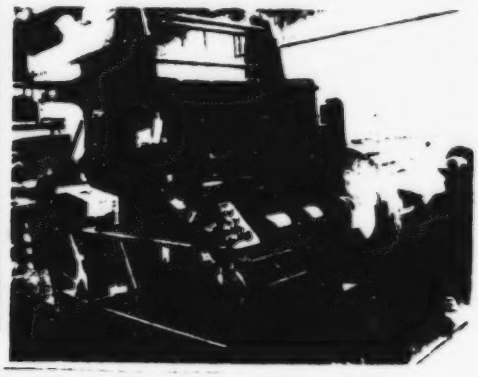

Figure 14: View of the aluminum foil parting machine where the on-line pinhole sensing device has been installed.

several kilometers are continuously passed through the machine. The minimum thickness, typically 10 μm, to which the foil can be milled is determined by a number of process parameters such as the material's malleability, the roller speed and surface quality, etc. When approaching the minimum allowed foil thickness, small pinholes start to form across the sheet. The density of such pinholes, which for certain applications must be guaranteed to be below a given value per unit area, is an important quality control parameter in aluminum mills. To this purpose, inspectors routinely cut a sample of foil from each reel, hold it against a bright background to obtain an image of the kind shown in Figure 15, and count the visible pinholes. Benefits of a statistical quality control range from product classification to meet the needs of different customers, to the tracking of specific process problems such as inadequate raw materials, roller surface damage, etc.

Continuous, on-line pinhole density monitoring is seeked to increase the inspection efficiency and surface coverage (the off-line inspector only has access to the last portion of each reel), as well as to avoid costly piling up of reeled product waiting for clearance. A miniaturized pinhole counting prototype was thus developed at our institute and in-process tested. A photo and diagram of the U-shaped sensor mounted at the foil splitting section of the aluminum foil parting machine is shown in Figure 16. A 0.1 mm x 5 mm line is projected on the foil with its longer axis oriented along the cross-machine direction, and any transmitted light is collected on a large-area photodetector. Figure 17 shows the time-resolved signal obtained during the laboratory calibration stage of the sensor with a calibrated pinhole of 50 μm in diameter. The sinc-square pulse shape corresponds to the rectangular slit beam-projection unit used in this prototype. Pinholes of 12 μm in diameter could be

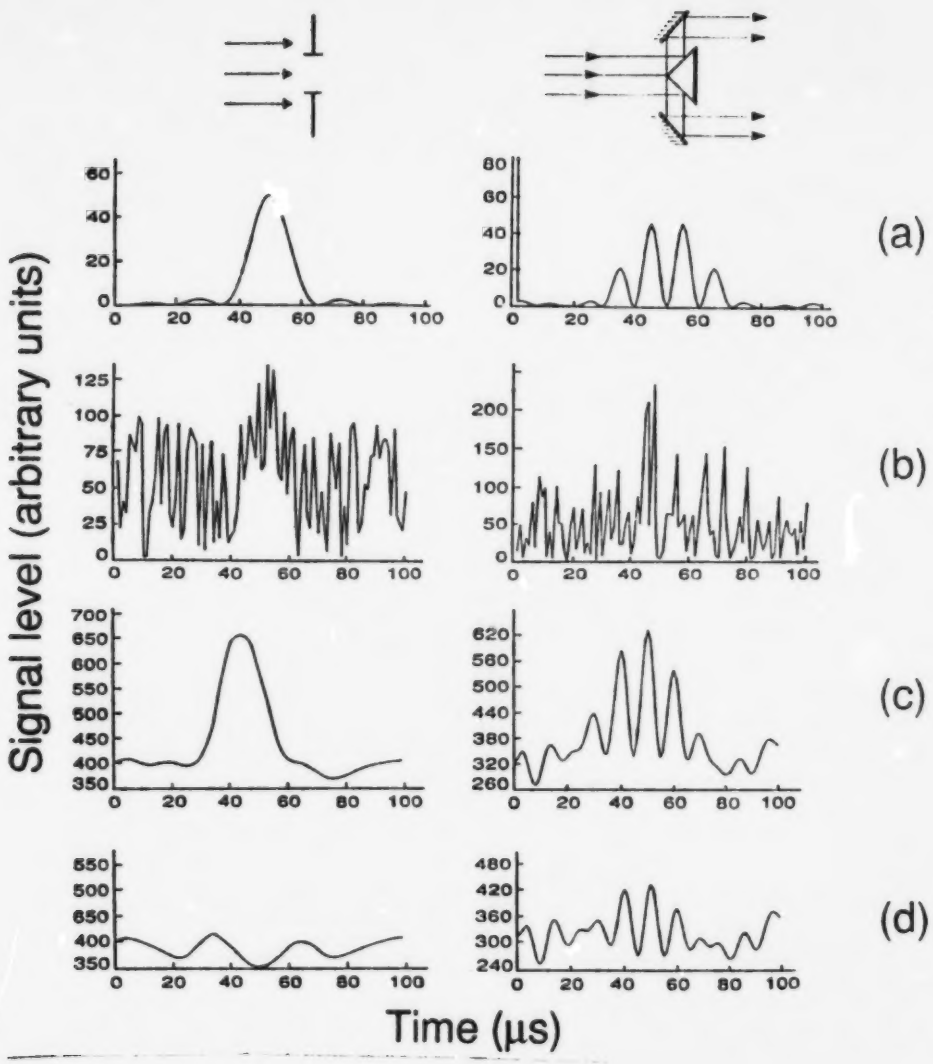

Figure 13: Simulated waveforms obtained with a beam shaping unit consisting of either a slit (left), or an interference fringe pattern projector (right), as detected (a) without noise, (b) with additive random noise, (c) after convolutional filtering, and (d) after filtering when only the noise is present.

detected with a signal/noise ratio higher than 10. Figure 18 shows an example of a signal obtained during the in-process tests with the foil running at 6 m/s. A double-pinhole defect can be clearly recognized in this case.

SPECKLE AVERAGING TECHNIQUES FOR ROUGH SURFACE INSPECTION

In the developments described above we have not been overly concerned about speckle noise. Speckle will appear only if the interaction with the inspected material introduces a random phase component on the laser beam. No such random phase will be produced when the beam is transmitted through a defect-free glass sheet or a clear-through pinhole. However, speckle effects do introduce a random modulation on the signal scattered by surface scratches or by irregularly shaped pinholes. This introduces a random component on the amplitude of the signal scattered by a defect, with a consequent decrease of the defect detection reliability if simple thresholding techniques are used for signal processing. Even in the cases

Figure 15: Typical pinhole pattern over a 15 cm x 20 cm aluminum foil surface.

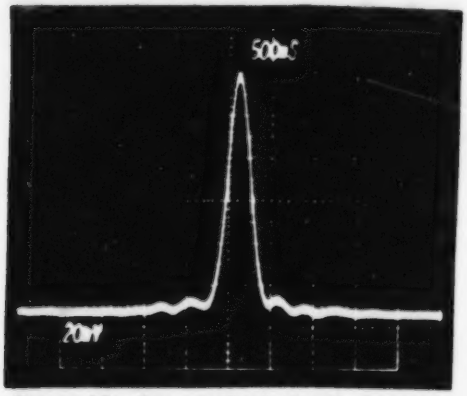

Figure 17: Time resolved signal obtained during the laboratory calibration of the sensor with a pinhole of diameter equal to 50 μm.

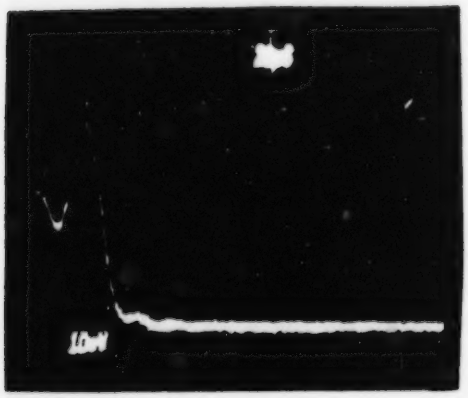

Figure 18: A double-pinhole signal obtained during the in-plant trials of the sensor mounted on the foil-parting machine during operation at 6 m/s.

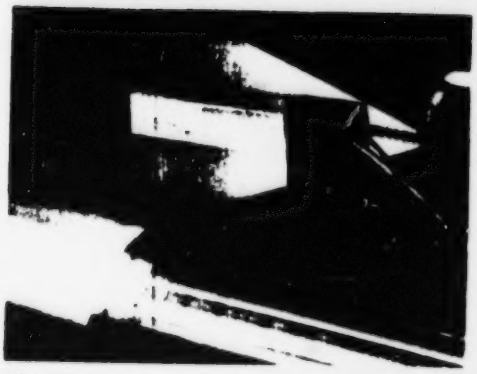

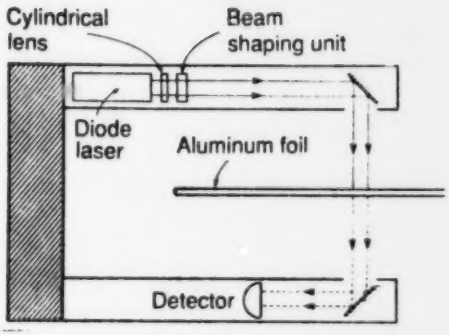

Figure 16: Top: head of the pinhole counting sensor installed on the aluminum foil parting machine shown in Figure 14. Bottom: schematic diagram of the sensor head.

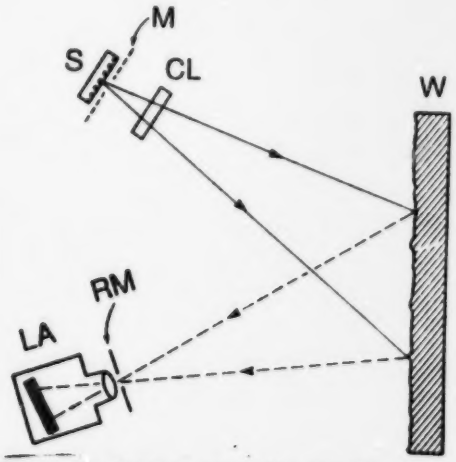

Figure 19: Optical setup for speckle noise investigations. S: laser source; M: variable mask; RM: rectangular mask; CL: cylindrical lens; W: rough-surfaced workpiece; LA: line-array camera.

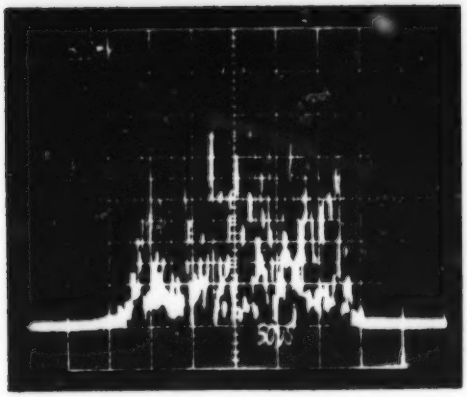

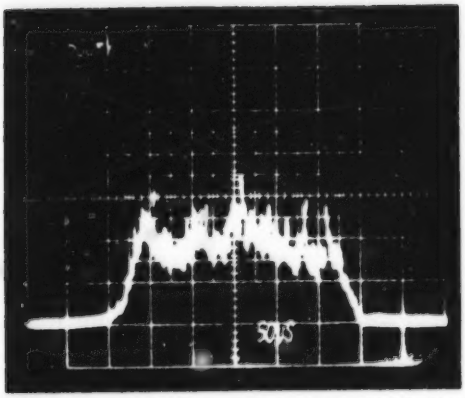

Figure 20: Line-array camera outputs obtained using the setup shown in Figure 19 with a He-Ne laser source and a camera aperture of (top) F/22 and (bottom) F/1.4.

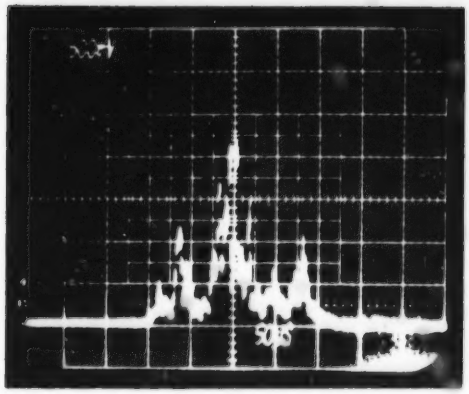

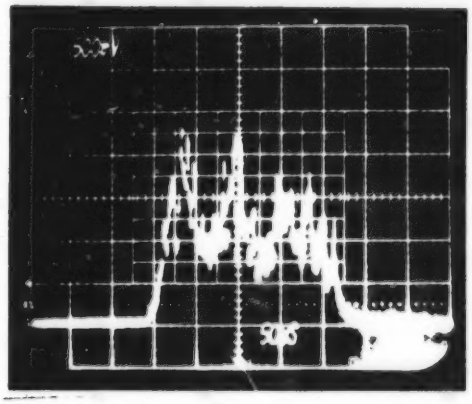

Figure 21: Line-array camera signals obtained under conditions similar to those of Figure 20(top), but using an incoherent diode-laser array source with either (top) one or (bottom) six light emitting segments being allowed to illuminate a given line on the inspected surface.

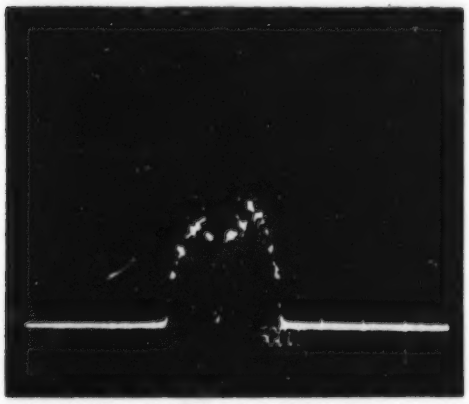

Figure 22: Line-array output similar to Figure 21(b), but obtained with a wide-aperture line array and a rectangular mask in front of the camera lens. A well resolved black-speck defect is visible in the middle of the illuminated line.

reported above, then, methods to reduce speckle noise would be welcome.

Speckle fluctuations are most visible when inspecting optically rough surfaces. Figure 19 shows an optical configuration where speckle noise is put in evidence. A rough object, in our case an unpolished aluminum sheet, is line-illuminated by a polarized laser source through a cylindrical lens whose axis is parallel to the plane of the figure. The nearly 10 mm x 100 μm line projected on the surface is imaged by a lens of variable aperture on a line-array photodetector with optical demagnification of nearly 2.5. Under such conditions, speckle grains should be visible on the camera image with average size (Ref. 1, Sect. 3.10):

$$d = \lambda \ell / D \qquad (1)$$

where λ is the wavelength, ℓ the lens-to-detector distance, and D the lens aperture. In our case, with $\lambda = 0.8$ μm and ℓ slightly larger than the lens focal length, the average diameter of the speckle grains on the photodetector-array plane is thus nearly equal (in μm) to the lens F-number.

If a perfectly coherent He-Ne laser source is used for line projection, line-array camera outputs of the kind shown in Figure 20 are obtained. If an F/22 aperture is used, i.e. a lens diaphragm of nearly 2.5 mm diameter with our 50 mm lens, speckle grains of typically 22 μm average size are expected as discussed above. This is of the same order of magnitude as both the width of the line image on the photodetector plane and the size of each 13 x 13 μm sensing element of the photodetector array. No spatial integration over adjacent speckle grains is thus performed by the camera in this case, so that speckle noise with r.m.s. amplitude fluctuations as large as the average signal intensity are expected, as confirmed by the output signal shown on the top of Figure 20. Evidently, the magnitude of such intensity fluctuations over the image of a surface whose reflectivity is nominally constant makes the interpretation of the recorded signal practically impossible. This figure illustrates a major drawback of laser illumination in optical inspection systems for defect detection, severely outbalancing the advantages of brightness, depth of field and spectral purity outlined in the introductory sections above.

Speckle noise can be reduced by opening the viewing lens aperture, as shown in Figure 20 (bottom) where the aperture has been increased to F/1.4. According to the above discussion, we are expecting in this case a speckle grain size of the order of 1.4 μm, so that each line-array sensor element integrates the intensity of nearly N = 100 speckle grains. This results in an improvement of the signal/noise ratio (see Ref. 1, Eq. 3-25) by a factor of the order of $N^{\frac{1}{2}} = 10$, as shown by Figure 20 (bottom).

This seems to lead to the conclusion that we can suppress speckle noise by widening the sensor element size and/or the lens aperture. However, the sensor size cannot be increased above the limits set by the required spatial resolution. As to the lens aperture, it should obviously be increased as much as possible not only because of speckle considerations but also to maximize the optical throughput. Limits to the lens aperture are, however, set by depth-of-field requirements. Moreover, the statistical nature of speckle noise makes it particularly harmful when inspecting for very sparse defects: even if the r.m.s. noise is reduced as in Figure 20 (bottom), occasional signal excursions of amplitude comparable to the average signal level may occur which could be interpreted as sparse defects.

Methods to further reduce speckle noise in addition to whatever degree of noise compression can be achieved by widening the aperture are thus of primary interest in laser-illuminated optical inspection. We are reporting here on one such approach which we have investigated for line illumination using a coplanar incoherent laser array source.

As shown in Figure 19, an array of uncoupled laser sources may be superposed by a single cylindrical lens to produce the illuminated line on the surface of the workpiece. If such laser sources are mutually incoherent, the speckle noise amplitude will be further reduced by a factor $N^{\frac{1}{2}}$, where N is the number of sources in the array. This is obtained without any compromise on the spatial resolution, spectral purity or depth of field if the laser array is coplanar with the projected laminar beam and if the width of each source in the direction normal to the projection plane is diffraction limited. It should be stressed that speckle averaging will take place only if the laser sources along the array are mutually incoherent. Evanescent-wave coupled laser arrays of the kind produced, e.g., by Spectra Diode Labs would not be appropriate for speckle reduction purposes.

An incoherent laser diode array obtained from the model LP2A by Laser Diode Products was used in our experiments to verify the above concepts. This array comprises 30 laser diode sources along the same 1.2 mm-long light-emitting junction of the GaA As semiconductor chip. The laser diodes, emitting a total power of 1 watt CW, are clustered in 6 light-emitting segments each containing 5 laser diodes. Although the 6 different segments are mutually incoherent, the 5 lasers within each segment are evanescently coupled so that the

speckle reduction factor will only be equal to $M^{\frac{1}{2}} = 6^{\frac{1}{2}} = 2.5$. in our case. A more efficient speckle compression would be obtained with fully uncoupled laser diode arrays, which are not yet, to our knowledge, commercially available, or by assembling fiber-optic arrays with individually fiber pigtailed laser diodes (see, e.g., Ref. 8, Fig. 8 or Ref. 9, Fig.20). The experiment reported here is, however, appropriate for a verification of the basic principle.

Figure 21 shows the speckle-modulated output obtained with the setup shown in Figure 19 using the laser diode array described above as the light source and an F/22 camera aperture. By varying the shape of mask M (see Figure 19), either a single segment of 5 laser diodes or the full array of 30 laser diodes may be made to contribute to the line illumination over the workpiece. The corresponding line-array outputs are shown in Figure 21 (top) and (bottom), respectively. As it can be seen, the speckle-generated signal modulation is substantially reduced when 6 uncoupled sources are superposed, in agreement with the above discussion.

Further noise reduction would be possible, at the expense of the depth of field, by widening the lens aperture, as illustrated in Figure 20. An increase of the lens throughput without compromising on the depth of field can be achieved, taking advantage of our line-illumination geometry, by inserting an asymmetric aperture in front of the camera lens. Using a wide-aperture linear array photodetector[10] and a lens aperture elongated in the direction perpendicular to the laminar beam plane, the depth of field in such a plane is insured by the small width of the slit aperture while the depth of field in the perpendicular direction is preserved by the narrow width of the projected laminar beam. Figure 22 shows the results of such a design. A line-array camera with 25 μm x 2.5 mm sensing elements, with a rectangular mask of 2 mm x 30 mm in front of the lens was used in a configuration of the kind shown in Figure 19 with 6-segment line illumination. Shown in Figure 22 is the line-array output with evidence of a 0.5 mm x 0.5 mm black speck defect in the center of the illuminated line. The spatial resolution was satisfactory over a 5 mm depth of field, the same depth as with the F/22 lens aperture. It can be seen, by comparison of Figure 22 with Figure 21(bottom), that the speckle noise has been considerably reduced by using the rectangular mask.

The obtention of high illumination power densities while complying with eye safety requirements is an additional advantage of using an uncoupled laser array. Although single diode lasers of CW power up to 1 W are available, which would produce a very intense power density along the projected line, such powers are not recommended because of eye safety problems. Laser intensities higher than 1 mW/cm^2, if inadvertently irradiating a human eye for durations exceeding 1 second, may exceed the maximum permissible exposure for safety (Ref. 1, Fig. 3-18b). Eye hazard is related to the high collimation of a coherent laser beam, which may be focused into a very small spot on the retina, eventually causing hole burning and localized blindness. The use of an array of uncoupled laser emitters of relatively low power correspondingly increases the power density along the projected line while keeping the power density of each spot image in the retina of the observer at a safely low level.

Finally, it should be mentioned that, although illustrated with reference to speckle compression when inspecting rough surfaces, the use of an uncoupled laser array is also beneficial in systems of the kind shown in Figures 6, 10 or 12 above. In the transmission configuration shown in Figure 6, a multiple-element source reduces, through angular averaging, the amplitude of signal fluctuations of the kind shown in Figure 7, which are generated by Fresnel lens indentations. In a scattering configuration of the kind shown in Figure 10, such a source reduces speckle noise in the scattered light field produced by rough-surfaced scattering defects, while in a pinhole-detection system as shown in Figure 12, incoherent laser superposition reduces the risk of "blind spots" along the projected laminar beam which may be produced by speckle fluctuations generated by dirt accumulation on the optics or by lens imperfections as shown in Figure 8(a).

CONCLUSION

A laminar-beam laser illumination method for on-line optical inspection has been described and a few applications to the inspection of industrial materials have been discussed. The interest of such an approach as compared to more conventional illumination techniques will now be summarized.

An inspection system using incoherent illumination avoids speckle noise but is affected by a number of problems including reduced illumination power density, limited depth of field, and lack of spectral discrimination possibilities to reject ambient noise. Laser mechanical scanning offers high instantaneous power, strong immunity to ambient light, long depth of field and convenient air purging through a slit. However, such a configuration requires a delicate mechanical scanning device subject to long-term wear, is subject to speckle noise, and needs a very high speed detector to resolve each pixel during a line scan. The

multiple-laser line illumination approach described in this paper does not require any moving scanner, is moderately affected by speckle noise, allows each detector element to integrate the collected light intensity during a relatively long period, of the order of the line scanning time, so that the required detector speed is modest, and assures better eye safety than a single high-power scanning laser. As compared to the incoherent illumination and video imaging approach, our configuration offers monochromatic laser light from which ambient light can easily be separated by optical filtering, long depth of field because of the small angular aperture of the projected laminar beam, convenience of air purging, strong laser illumination, one-dimensional scanning much faster than the readout of a two-dimensional matrix-array camera, and higher transverse resolution with a standard 2048 element line array as compared to a typically 480 x 550 element camera.

The authors gratefully acknowledge the skilled assistance of F. Levesque for the installation of the glass panel inspection system.

REFERENCES

1. P. Cielo, Optical Techniques for Industrial Inspection. Academic Press, Boston (1988).
2. G.M. Clarke and J. Bedford, "Laser scanning for defects, dimensions and surface finish" Proc. 3rd Int. Conf. on Automatic Inspection and Product Control, Nottingham, p. 119, IFS, U.K. (1978).
3. T. Matsubara, T. Toyota and A. Fujiyama, "Hot slab inspection by the laser scanning method" in: Optical Techniques for Industrial Inspection, P. Cielo Ed., Proc. SPIE, Vol. 665, p. 17 (1986).
4. D.J. Purll, "Assessment of silicon imaging array performance" in: Image Assessment: IR and Visible, T.L. Williams Ed., Proc. SPIE, Vol. 467, p. 122 (19823).
5. J.R. Hador, T.J. Schapp and N.E. Buholtz, "Experimental characterization of linear imaging arrays" in: State-of-the-art Imaging Arrays and their Applications, K.N. Prettyjohns Ed., Proc. SPIE, Vol. 501, p. 202 (1984).
6. P. Cielo, M. Dufour and A. Sokalski, "Optical inspection in hostile industrial environments: single-sensor vs. imaging methods" in: Optomechanical and Electro-optical Design of Industrial Systems, R.J. Bieringer and K.G. Harding Eds., Proc. SPIE, Vol. 959, paper 07 (1988).
7. D.J. Purll, "Automated surface inspection with solid-state image sensors" in: Industrial Applications of Solid-state Image Scanners, D.J. Purll Ed., Proc. SPIE, Vol. 145, p. 18 (1978).
8. P. Cielo, G. Vaudreuil and M. Lamontagne, "In-process product control by electro-optical sensors" ISA-Digicom '87 Conference, Montreal, Oct. 21-22, (1987).
9. P. Cielo, M. Lamontagne and G. Vaudreuil, "On-line electro-optical instrumentation for continuous quality control of manufactured sheets" ISA Trans., Vol. 27, p. 31 (1988).
10. P. Cielo and M. Lamontagne, "Improvement of subpixel resolution in triangulation ranging by astigmatic spot projection and wide-aperture line array imaging" Opt. Laser Techn., Vol. 20 (1), p. 19 (1988).
11. A.J. Barker and R.A. Brook, "A design study of an automatic system for on-line detection and classification of surface defects on cold-rolled steel strip" Opt. Acta, Vol. 25, p. 1187 (1978).